

Experiment 21
A BETA SPECTROMETER AND RELATIVITY

A TEST OF RELATIVITY	1
Momentum-energy relation for fast electrons: Newton v. Einstein.....	1
Using a magnet to determine momentum	2
BETA DECAY AS A SOURCE OF FAST ELECTRONS	3
¹³⁷ Cs radioactive beta decay.....	3
Internal conversion.....	4
Beta decay and the neutrino	5
EXPERIMENTAL APPARATUS	7
Magnetic focusing of the electrons	7
The Hall Probe and its calibration	9
Silicon diode particle detector	10
Pulse-processing electronics	12
PROCEDURE	13
Energy calibration.....	14
Pump down the vacuum chamber	14
K line magnetic field measurements.....	15
Acquire β electron magnetic field v. energy data	16
Secure the apparatus.....	16
PRELAB PROBLEMS	17
ANALYSIS	19
APPENDIX A: USEFUL NUMERICAL DATA	A-1
¹³³ Ba calibration source.....	A-1
¹³⁷ Cs conversion electron energies.....	A-1
Compton edge energy calculation.....	A-1
Silicon detector γ -photon sensitivity data	A-2

A BETA SPECTROMETER AND RELATIVITY

By using a focusing magnet and energy-sensitive detector, the momenta and the corresponding kinetic energies of fast electrons may be compared. You will use this momentum-energy data to test one of the predictions of *Special Relativity*. Radioactive beta decay of ^{137}Cs nuclei provide the electrons, whose kinetic energies range up to approximately 1 MeV; at these energies the difference between the predictions of the Newtonian and relativistic theories of motion should be quite clear. The experiment will also provide you with a better understanding of the radioactive beta decay process as well as provide a bit of experience with solid-state particle detector technology and its associated electronics.

A TEST OF RELATIVITY

To get the most from the following discussions of the relativistic electrons' momentum-energy relations, you might want to review the material in *General Appendix A: Relativistic Kinematics* – particularly those sections up through *Kinetic energy* and equation (A-9) on page A-4.

Momentum-energy relation for fast electrons: Newton v. Einstein

Newtonian mechanics specifies a simple relationship between a particle's linear momentum \vec{p} and its kinetic energy T due to that motion: $p^2 = 2mT$. The relation between the momentum and the kinetic energy of a particle according to relativity theory, on the other hand, is given by:

$$p^2 = 2mT \left(1 + \frac{T}{2mc^2} \right) \quad (21-1)$$

The derivation of equation (21-1) is left to the Prelab Problems. The extra term $T/2mc^2$ in this expression implies that the momentum of a particle grows more rapidly with kinetic energy than the Newtonian theory would predict, especially as the particle's kinetic energy

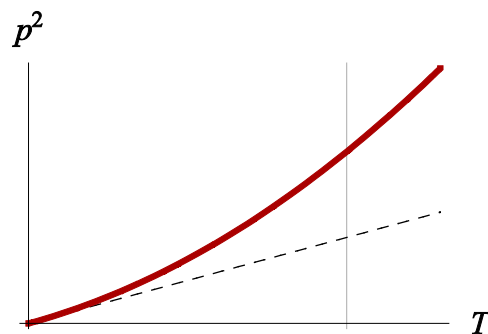


Figure 1: Special relativity predicts that the growth in momentum p with increasing kinetic energy T is more rapid than the Newtonian prediction (dashed line). At $T = 2mc^2$ (vertical reference line), the relativistic p^2 is twice the Newtonian value.

becomes comparable to its *rest energy*, mc^2 (see Figure 1).

Using a magnet to determine momentum

A charged particle in a magnetic field will experience a *Lorentz force*¹ due to the field given by (SI units):

$$\frac{d}{dt}\vec{p} = \vec{F} = q\vec{v} \times \vec{B} \quad (21-2)$$

This expression is correct for both Newtonian and relativistic descriptions. Since the magnetic force is orthogonal to the direction of motion of the particle, it does no work on the particle and cannot change the particle's kinetic energy. Thus a charged particle's speed in a magnetic field remains constant; only the particle's direction of motion can change. A particle whose velocity is orthogonal to a uniform, constant magnetic field will thus follow a circular path of radius r in a plane normal to the field with centripetal acceleration $\dot{v} = v^2/r$. Relating this acceleration \dot{v} to the force F given by (21-2), you can derive the following SI expression for the radius r of the particle's circular motion, known as the *Larmor radius*²:

$$r = \frac{p}{qB} \quad (21-3)$$

Thus if you know the radius of curvature of a charged particle's motion through a uniform magnetic field, then you can determine its momentum using (21-3). This may be accomplished using a magnet with the configuration shown schematically in Figure 2. Arranging the source and detector as shown with respect to the cylindrical area containing the magnetic field B ensures that only particles with a Larmor radius equal to R_{eff} will arrive at the detector. How such an arrangement also serves to focus the beam of charges is described below (starting on page 7); a more thorough description, including more realistic magnetic field modeling, is available in the notes to *Physics 6 Experiment 9: A Mass Spectrometer*.

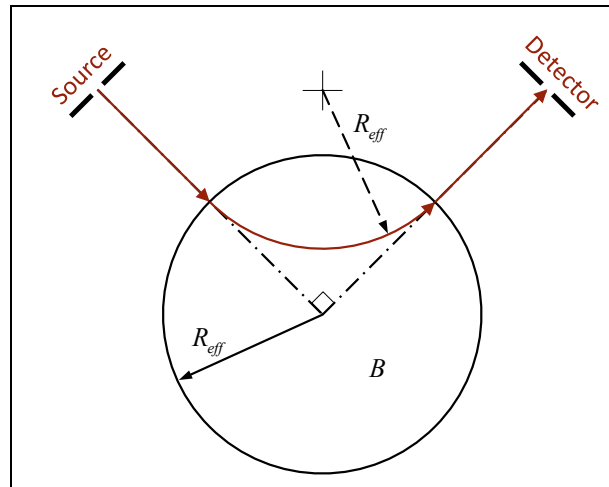


Figure 2: Schematic arrangement of the electron path through the magnetic field. The direction of B is normal to the plane of the figure. The particles enter and exit the field along radius vectors separated by 90° .

¹ The Dutch physicist Hendrik Lorentz published his derivation of the complete electromagnetic force law $\mathbf{F} = q(\mathbf{E} + \mathbf{v} \times \mathbf{B})$ in 1895, although a statement of the magnetic contribution to the force was first published by Oliver Heaviside in 1889.

² Named for British physicist James Larmor, an important figure in the electrodynamics of moving charges and the early development of what became the theory of relativity.

By controlling the magnetic field strength B , the experimenter determines the momentum p of those electrons which can reach the detector using equation (21-3) with $r = R_{eff}$. The detector in Figure 2 must be able to determine the arriving electrons' kinetic energy T ; this combined momentum-energy data then provides the means to compare the relativistic expression (21-1) to the simpler Newtonian theory.

BETA DECAY AS A SOURCE OF FAST ELECTRONS

¹³⁷Cs radioactive beta decay

The electron source used for this experiment is a radioactive ¹³⁷Cs sample³, which is convenient both because it has a relatively long half-life (30 years), and because it emits fairly high-energy electrons (kinetic energies on the order of an MeV). You investigated the high-energy photon emission from ¹³⁷Cs when you performed Experiment 30, but the radioactive material used in those samples is sealed in a thick plastic matrix so that the electrons emitted from the decaying atoms cannot escape. In this experiment the samples *are not sealed* so that the electrons do escape and can enter the apparatus. Let us review the ¹³⁷Cs → ¹³⁷Ba decay scheme, Figure 3.

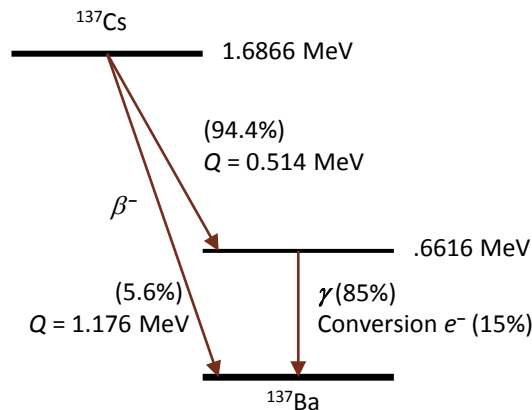


Figure 3: Decay scheme for ¹³⁷Cs. The electrons from beta decay (β^-) and internal conversion transitions will be used for this experiment. Level energies are relative to the ¹³⁷Ba ground state; β^- electron maximum kinetic energies (Q values) are also listed.

Beta decay of ¹³⁷Cs usually leaves the daughter nucleus (¹³⁷Ba) in an excited state which subsequently decays to its ground state either through γ -ray emission or through *internal conversion* (ejecting an atomic electron in the process).

³ ¹³⁷Cs is produced by fission of ²³⁵U in nuclear reactors; it has been a most problematic contaminant following the nuclear power plant disasters at Chernobyl and Fukushima.

Internal conversion

A typical excited daughter nucleus following radioactive decay loses its excess energy via photoelectric emission – emission of one or more γ -photons as the nuclear state cascades downward to its ground state. In the case of ^{137}Ba , however, a significant fraction of the time (15%) the excited nucleus reaches its ground state through the more exotic process of *internal conversion*.

A transition between two states may be difficult for a system to accomplish through *photon emission* for a variety of reasons: for example, the charge configurations of the two states may be such that the external electromagnetic field doesn't change much as a result of the transition (a $2s$ - $1s$ electron transition in atomic hydrogen, for example); or, for another example, the angular momentum difference between the two states may be so large that it is difficult for a single photon to carry away the excess – this happens to be the case for the 0.6616 MeV nuclear state in ^{137}Ba , where the difference in the angular momentum quantum numbers of the two states is $\Delta J = 4$. Such transitions are generally referred to as *forbidden transitions*, and the lifetime of the excited state in such a situation can be very long – the phenomenon of *phosphorescence* being a common atomic or molecular example.

A nucleus can sometimes rid itself of this excess energy and reach its ground state by transferring the energy to an atomic electron using the Coulomb force between it and that electron; the electron can then efficiently carry away both the excess energy and the angular momentum the nucleus needs to lose. Because the relatively light electrons experience such a strong Coulomb force when they enter the nucleus (56 protons in a barium nucleus, all packed within a couple of *femtometers* [10^{-15} m] radius), their consequent accelerations can be quite large. This is the essence of the internal conversion process, and an atomic electron ejected from the atom following this energy transfer is called a *conversion electron*. Picture this process as a quantum analog of how NASA gets probes to the outer solar system by whipping them around inner planets to pick up kinetic energy from the planets' orbital motions.

For an electron to participate in the internal conversion energy transfer it must approach very close to the nuclear protons – only those electrons whose atomic wave-functions have significant amplitude at the nucleus need apply. This restriction limits the choice to the electrons in $1s$ or $2s$ orbitals, with the $1s$ electrons having significantly higher probability (the higher-energy s -orbital electrons might also participate, but with very small probability). The electrons occupying $1s$ orbitals are known in the atomic spectroscopy parlance as K electrons; those in $2s$ as L_1 (or, simply: L) electrons.

Following the receipt of the nuclear energy transfer (0.6616 MeV in our case), the electron must climb out of the Coulomb potential well of the nucleus, losing an amount of kinetic energy equal to its *atomic binding energy*. Since the K ($1s$) electrons are much more strongly bound than the L electrons (more than a factor of 6 in the case of barium), a K conversion

electron will have lower kinetic energy following its escape from the atom than will an L electron.

Although some escaping conversion electrons may also lose a random amount of additional kinetic energy by colliding with other atomic electrons (causing additional ionizations), for the most part the conversion electrons from a given shell (K or L) are *monochromatic* or *monoenergetic*: they have well-defined kinetic energies equal to the nuclear energy loss minus the electron binding energy.

Beta decay and the neutrino

The radioactive decay of ^{137}Cs happens when one of the nuclear neutrons changes to a proton and *an electron is created* (out of thin air!) which balances the new proton's electric charge. This brand new electron then escapes the nucleus as a so-called *beta particle*.⁴ Although the energy lost by a nucleus during β -decay is well-defined (being the difference in the parent and daughter nuclear masses), the escaping β electrons were observed to have a continuous spectrum of possible kinetic energies up to this well-defined nuclear mass difference (minus the electron's rest mass), as shown in Figure 4.

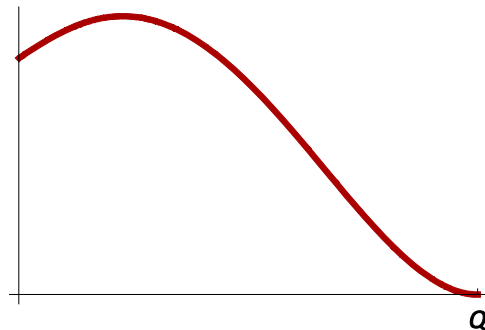


Figure 4: Typical spectrum of β electron kinetic energies. The relative probability of observing a decay event with a specified β electron kinetic energy is plotted v. that energy (Q is the maximum observed kinetic energy).

This apparent failure of energy conservation in the case of β -decay seemed to be accompanied by an equally-troubling violation of conservation of angular momentum: since the total number of nucleons (protons and neutrons) is not changed during the decay, the new electron's intrinsic spin of $\frac{1}{2}$ could not be balanced by a compensating change in the decay products' other sources of angular momentum (whose total can only change by an integer number).

⁴ Alpha and Beta radiation were named by the British physicist Ernest Rutherford in 1899. The French physicist Henri Becquerel confirmed that the beta particle's charge/mass ratio is the same as that of the electron in 1900. Rutherford was awarded the 1908 Nobel Prize in Chemistry for his pioneering discoveries about radioactive decay; Becquerel, the discoverer of radioactivity, shared the 1903 Nobel Prize in Physics with Marie and Pierre Curie.

A solution to this dilemma was proposed by the then-Austrian physicist Wolfgang Pauli (of *Pauli Exclusion* fame) in 1930: an unobserved, electrically neutral particle is also created along with an electron during β -decay. This spin- $\frac{1}{2}$ particle would share the decay's energy with the electron so that the sum would equal that lost by the nucleus; because of the various possible escape directions of the two particles, linear momentum conservation would divide the available energy in various ways among the two particles, accounting for the observed electron kinetic energy spectra (Figure 5). After discovery of the neutron in 1932⁵, Pauli's hypothesized particle was rechristened the neutrino by Enrico Fermi⁶. The neutrino⁷ was finally detected experimentally in 1956 by the Americans Clyde Cowan and Frederick Reines⁸.

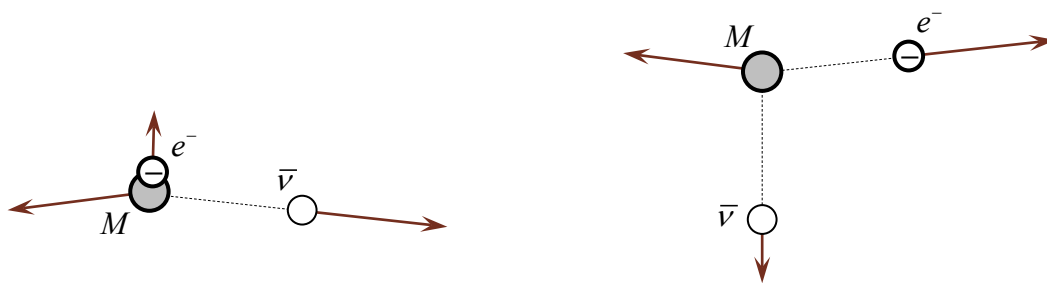


Figure 5: The geometry of the β -decay determines how the available kinetic energy Q is shared between the electron (e^-) and neutrino ($\bar{\nu}$) (actually an *antineutrino*); the arrows in the diagrams show the distribution of *linear momentum* among the particles (M is the nucleus). Left: in this example decay most of the available kinetic energy has gone to the neutrino; right: most has gone to the electron. Since the neutrino has almost no mass, its speed will nearly always be very close to the speed of light, even when it gets only a relatively small amount of the available energy.

This continuum of possible β electron energies (Figure 4) makes the ^{137}Cs decay a useful source of a multitude of electron energies and momenta to test the relativistic expression in equation (21-1).

⁵ The neutron was discovered by the English physicist James Chadwick in 1932, while with Rutherford at Cavendish Laboratory in Cambridge. His discovery earned him the 1935 Nobel Prize in Physics.

⁶ The Italian physicist Enrico Fermi developed a comprehensive and truly pioneering theory of beta decay in 1934. His subsequent development of the first nuclear reactor and his discoveries therewith earned him the 1938 Nobel Prize in Physics.

⁷ The neutrino was thought for many years to be a massless particle, but current experimental evidence indicates that it has a nonzero, albeit tiny, rest energy. Studies of the β -decay of tritium and of the so-called neutrino oscillations, as well as recent cosmic microwave background studies currently place the neutrino's rest energy at somewhat less than $\frac{1}{2}$ eV, more than a million times smaller than that of the electron.

⁸ Cowen and Reines began their experiments in 1951, searching for neutrinos emitted by a nuclear reactor. Reines was awarded the Nobel Prize in Physics for their discovery in 1995 (Cowan had died in 1974).

EXPERIMENTAL APPARATUS

A typical arrangement of the β spectrometer apparatus is shown in Figure 6 with its major system components labeled. Selected systems will be discussed in more detail in the following sections.

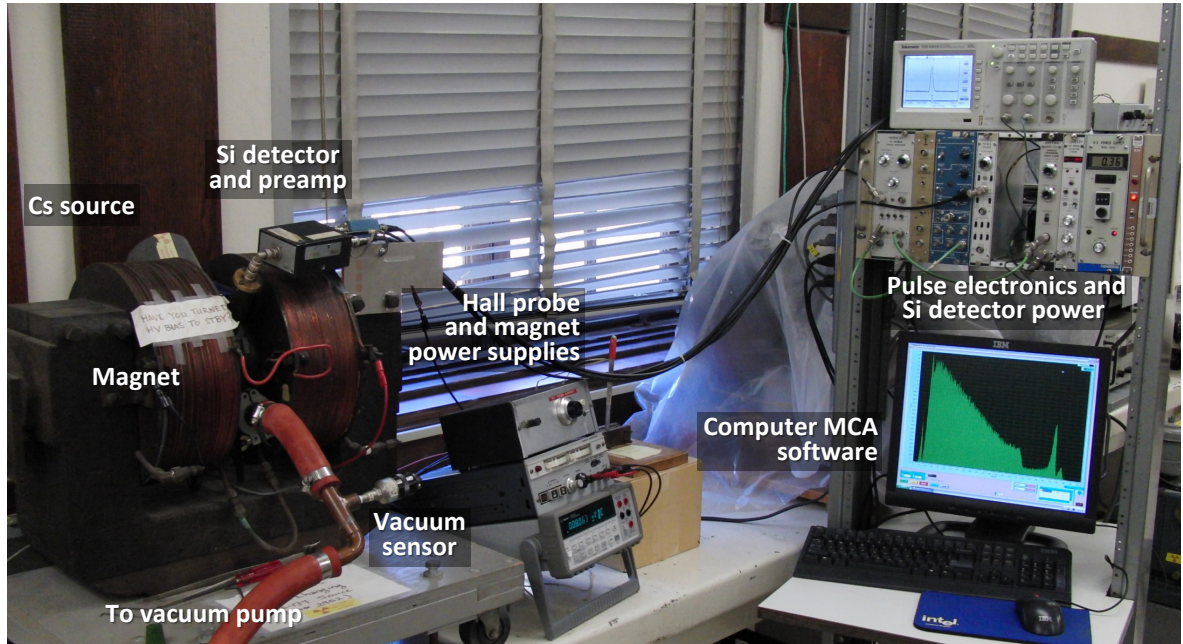


Figure 6: The β spectrometer apparatus with its typical electronic equipment arrangement. The experimenter uses the computer to control MCA energy spectrum acquisition, while the magnetic field is set using the magnet power supply and Hall probe field strength measurement.

Magnetic focusing of the electrons

The magnetic field not only selects the momentum of the electrons to be detected, as described previously (see page 21-2 of the notes), it also provides focusing of the electrons (for the selected momentum) between the ^{137}Cs source exit slit and the detector entrance slit as we shall now describe. For this discussion we use a simplified model of the magnetic field which is uniform within a radius R_{eff} of the pole axis and 0 elsewhere, as shown in the figures. Consider Figure 7; we know that upon entering a region with a constant, uniform magnetic field, each electron will follow a circular path with constant speed and the constant radius given by (21-3). In order to make the 90° turn shown in the figures, this radius must match R_{eff} . This condition will clearly route electrons which enter the magnetic field exactly along a radius vector of the field region to an exit along another radius vector displaced by 90° (this central path from source to detector was shown in Figure 2 and is again displayed in Figure 7).

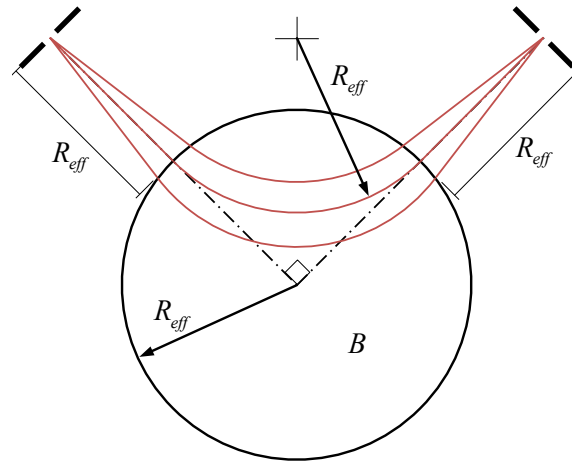


Figure 7: A diagram of the path electrons take from the ^{137}Cs source (upper right) to the Si diode detector (upper left). The electrons are turned through 90° and focused by the magnetic field B , which is perpendicular to the plane of the figure. With the geometry shown, focusing is accomplished only for those electrons whose Larmor radius is equal to the effective radius of the magnetic field, R_{eff} .

What we wish to demonstrate is that, with proper positioning of the source and detector, electrons whose paths from the source differ slightly from this ideal will still be directed to the detector: the magnet also serves to *focus* the electrons onto the detector slit. To proceed with this analysis set up an x - y coordinate system for the plane of the electrons' path with its origin at the pole axis, the x -axis aligned with the electron source slit, and the y -axis aligned with the detector entrance slit, as shown in Figure 8 (on page 21-9).

Selected electrons approaching the magnet exactly along the x -axis in Figure 8 follow a circular arc in the field with a center of curvature at $(x, y) = (R_{eff}, R_{eff})$. Now consider ions which are not approaching from exactly along the x -axis. One such electron may enter the field and follow a circular arc with its center very slightly displaced, i.e.: its center of curvature is at $(x, y) = (R_{eff} + u, R_{eff} + v)$, where u and v are both $\ll R_{eff}$. This situation (for positive u and v) is depicted in the figure. We ask the following questions: could such an electron have originated from a point on the x -axis, and if so, how far is this point from the magnet, and similarly could its destination upon leaving the field be somewhere on the y -axis?

A review of Figure 8 while keeping in mind that u and v are small should convince you that angles θ and ϕ are also small, so we can approximate $\theta \approx v/R_{eff}$ and $\phi \approx u/R_{eff}$. Thus we have the similar triangles shown, and clearly the offset electron path intersects the x and y axes with angles ϕ and θ , respectively. The distances from the edge of the magnetic field to the intersection points we call U and V , as also shown in the figure.

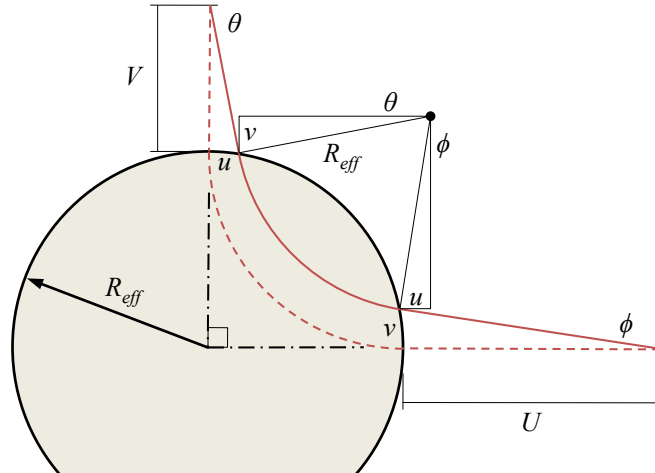


Figure 8: The geometry used to evaluate the focusing performance of the magnet.

Thus, in the limit of small θ and ϕ , $u/V = v/R_{eff}$ and $v/U = u/R_{eff}$. Eliminating u and v from these equations, we find that

$$UV = R_{eff}^2 \quad (21-4)$$

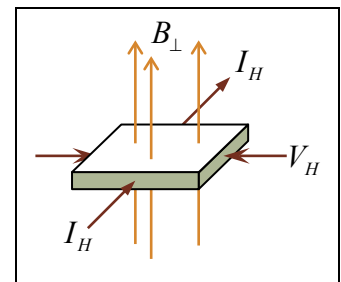
Equation (21-4) is independent of u and v (as long as they are small), so if the source is positioned at a distance U from the magnet, electrons emitted through a small range of angles will be focused at a point a distance V from the magnet, as shown in the figure! This formula may be cast into a form equivalent to that for a thin optical lens of focal length R_{eff} by using the distances from the origin to the two focal points, $U' = U + R_{eff}$ and $V' = V + R_{eff}$. With these definitions, (21-4) becomes:

$$\frac{1}{U'} + \frac{1}{V'} = \frac{1}{R_{eff}}$$

This ability to focus an electron beam also applies to more realistic magnetic field models; the interested reader should consult the notes for *Physics 6 Experiment 9* for details.

The Hall Probe and its calibration

A *Hall probe*⁹ is used to accurately measure the strength B of the magnetic field experienced by the electrons as they traverse the narrow gap between the electromagnet's two pole-pieces. Following probe calibration, you will position it in this gap on the pole-piece axis. The Hall probe sensor is a small, thin, rectangular semiconductor wafer. As illustrated in the diagram at right, current I_H from a power supply flows across the wafer from one edge to the opposite, and the voltage V_H across the other two edges is measured by



⁹ The American Edwin Hall discovered the effect now named for him in 1879.

a sensitive voltmeter. Ideally, the measured V_H is proportional to the product of the component of the magnetic field normal to the surface of the wafer, B_{\perp} , and the current I_H , because the Lorentz force causes the charge carriers in the wafer to be deflected by B_{\perp} toward one edge as they travel through it. This build-up of mobile charge carrier density along one edge in the (overall neutral) piece of material creates an electric field orthogonal to the direction of current flow, which is sensed by V_H .

You calibrate the hall probe in three steps:

- (1) Hold the probe far from any magnets and with its surface oriented parallel to the Earth's field. In this case we should have $V_H = 0$, but imperfections in the uniformity of the material of the probe will produce a residual voltage offset (which would result in a systematic error in your Hall probe measurements). Use the *offset null* function of the voltmeter attached to the probe to zero out this residual voltage reading, and thus mitigate this source of error.
- (2) Insert the probe into the calibration magnet (a small, permanent magnet) and adjust the Hall probe current I_H using the potentiometer on its power supply until the measured V_H corresponds to the value of the calibration magnet field B (for example, you would adjust I_H so that a calibration magnet field of 807 Gauss might correspond to a voltage reading of 8.07 mV, for a conversion factor of 100 G/mV).
- (3) Store the calibration magnet far (half a meter or so) from the electromagnet used for the experiment so that you don't inadvertently change its magnetization!

Make sure you record the calibration magnet's field value and its uncertainty (another systematic error source) along with the voltage you measured.

Silicon diode particle detector

To test the theory represented by equation (21-1), we also must determine the kinetic energies of the charged particles we send through the magnetic field shown in Figure 2. To accomplish this measurement, the apparatus uses a *silicon diode detector*. The physics of the semiconductor *PN junction diode* is discussed briefly in *Physics 6 Experiment 13: The Solid State Diode*; you may want to review that experiment's *Appendix: Elementary physics of the PN junction diode*.

The basic operation of a solid-state diode detector is as follows:

1. The diode is *reverse-biased* with a bias voltage of a few hundred volts, so in its idle state it conducts only a very small leakage current.
2. The large *depletion region* of the diode in this state is nearly empty of charge carriers: thermally-generated *electron-hole pairs* make up the only source of charge carriers, and these pairs are the source of the diode's small leakage current.

3. Any high-energy electron entering the diode's depletion region will collide with the silicon atoms' valence electrons, starting a cascade of ionizations which will quickly convert its initially large kinetic energy into the ionization of thousands of electrons removed from their parent silicon atoms.
4. These secondary electrons and the holes they left behind are swept from the diode's depletion region by its reverse bias voltage, resulting in a short pulse of current through the diode's external circuitry with a charge equal to that of the total charge of the freed electrons; this current pulse signal is integrated and amplified by the system electronics.

Of course, a high-energy photon entering the diode's depletion region can Compton scatter or be photoelectrically absorbed, releasing a high-energy electron which would subsequently generate a current pulse in the diode circuitry as described above.

The silicon diode detector has a major advantage over a scintillation detector for this experiment: the total charge of the ionized electrons released following a high-energy interaction is directly measured by the diode circuitry; thus the inefficiency of the scintillation-to-photomultiplier step is eliminated. There are typically hundreds of times as many electrons generated in the silicon detector (which determine the Poisson counting statistics), greatly enhancing its energy resolution over that of a sodium iodide crystal scintillator. The average energy required per electron-hole pair creation by a high-energy event in the silicon diode detector is approximately 3.8eV, compared to the several hundred eV required per photoelectron in a good NaI scintillation detector.

A slightly less important advantage of the silicon detector derives from its small size and the relatively low atomic number of silicon: its sensitivity to high-energy photons is not as great as for a NaI detector, reducing the γ -photon detection background and improving the signal-to-background ratio for electron detections. Luckily, the γ -photon sensitivity is high enough for us to use γ -ray sources for detector system energy calibration.

The silicon diode detector has one disadvantage, however. Since silicon's band-gap energy is a relatively small 1.1eV, random thermal generation of electron-hole pairs in the diode depletion region is a significant noise source; the large reverse bias voltage on the diode can even accelerate thermally-created charge carriers to sufficient energies to occasionally generate secondary ionizations as well. This background of random, although small, thermally-generated current fluctuations greatly reduces the detector's sensitivity to particles with energies of less than several tens of keV and also limits the detector's energy resolution by adding a random amount of thermally-generated ionizations to those caused by a high-energy particle detection. Cooling the detector could greatly improve the noise situation, but you will use it at room temperature in this experiment. In fact, cooled silicon detectors are often used to detect x-ray photons in the energy range of a few to about 100 keV.

Pulse-processing electronics

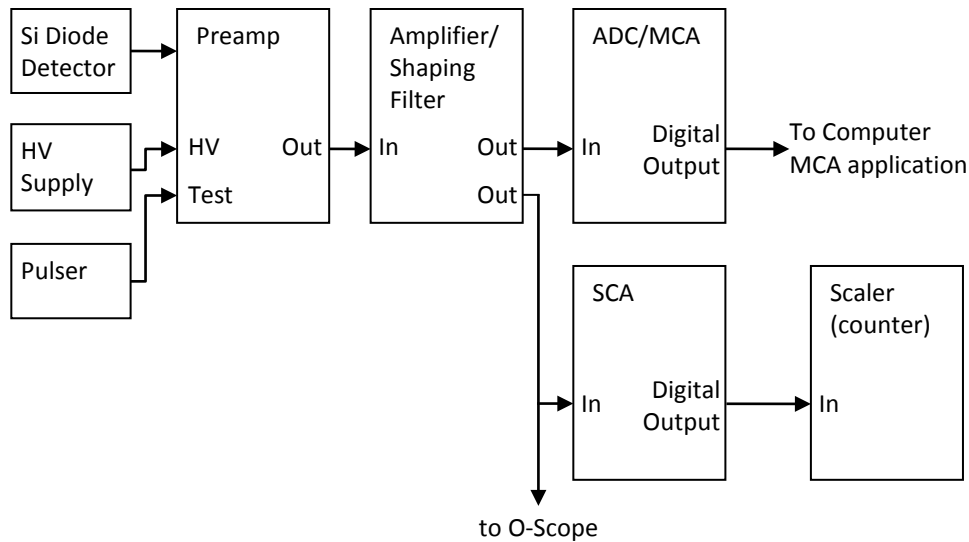


Figure 9: System-level diagram of the detector and pulse-processing electronics.

The pulse-processing electronics system (Figure 9) is functionally quite similar to that used with the NaI scintillators in Experiment 30a: current-integrating preamplifier → pulse-shaping, variable-gain amplifier → analog-digital converter (ADC) → MCA histogram display. In this experiment setup, however, each subcomponent in this sequence, as well as the diode's high-voltage power supply, is implemented by a separate electronics module. These individual modules provide for customization of a setup to suit the particular needs of an experiment such as this one. Many of the electronics components are designed to the *NIM* (nuclear instrumentation module) standard originally created in 1968, although it is still supported by several manufacturers even today. Because of this flexibility in the choice of components, the particular modules used to implement each function in the signal processing chain may be changed from time to time.

The current pulses from the silicon diode detector are integrated, converted to a voltage, and amplified by a current-integrating preamp. The preamp is mounted close to the detector (see Figure 6) because the diode's output signal is quite small (only about 3 *femtocoulombs* for a *K* conversion electron detection). The preamp output is shaped into a pulse and further amplified by an amplifier. You may adjust the fine gain of this amplifier to control the horizontal position of features on the MCA display as you did in Experiment 30a.

The high-voltage power supply (*HV Supply* in the figure) sets the reverse-bias voltage of the silicon diode detector. Setting the voltage too high will cause irreversible damage to the diode; the laboratory administrator will have preset the voltage to the proper value to optimize the sensitivity of the detector.

The *Pulser* shown in Figure 9 may be used to insert synthetic “event detections” into the electronics system for testing or to help the experimenter set gains and thresholds. When activated, it outputs a continuous series of identical pulses whose height may be set by a control on the device. You would normally set this pulse height so that the Pulser output mimics detections of some particular event (such as a *K* conversion electron); an oscilloscope attached to the amplifier output is particularly helpful to monitor the pulse voltage level.

The *SCA* (single channel analyzer) has two adjustable voltage thresholds: a lower and an upper level. If an input signal’s pulse height falls within the bounds set by these limits, then the SCA outputs a short digital pulse. Its output is connected to a *Scaler*, a device which counts the digital pulses presented to its input and displays a running total of the pulses counted. The experimenter may adjust the time interval over which the Scaler will accumulate counts.

PROCEDURE

Always **disable the high voltage bias** and disconnect the detector from the preamp whenever you change the configuration of the experiment (insert or remove ^{137}Cs calibration source, start or stop the vacuum pump, etc.).

Do not connect or disconnect the detector from the preamp unless the high voltage output is disabled!

Do not insert or remove the detector from the magnet apparatus while it is connected to the preamp!

Any change to the power supply output takes about 30 seconds to take effect because of the low-pass filtering internal to the signal preamplifier. Depending on the power supply in use, the high voltage output is disabled by selecting STANDBY or OUTPUT OFF or something similar – just ask your TA for assistance if needed. **Do not turn off the power supply power switch except as a last resort.**

The in-lab procedure is composed of the following steps:

1. Use the ^{137}Cs and ^{133}Ba calibration sources to familiarize yourself with the electronics and the MCA software and to acquire energy calibration spectra.
2. Pump the electron path chamber down to vacuum and calibrate the Hall probe.
3. Use the SCA and Scaler to accurately determine the magnetic field required to detect the *K* conversion electrons from the ^{137}Cs source.
4. Acquire β electron energy data for several different magnetic field settings for later analysis.

Energy calibration

Insert the ^{137}Cs calibration source into the apparatus using the special tool provided. After reconnecting the preamp to the detector, make sure that its back end is supported by the aluminum plate attached to the magnet; don't allow the detector connector to become the sole support of the weight of the preamp.

The HV Supply should already be adjusted to the correct high-voltage bias value (somewhere in the 250–400 V range); check with your TA or the lab administrator to confirm this. Apply the bias voltage to the detector and begin taking MCA energy spectra of the ^{137}Cs calibration source. Identify the K conversion electron line in the spectrum (refer to Figure 10 and your answer to Prelab Problem 1) and adjust the amplifier's *Fine Gain* to place the K line near MCA channel 400.

Now take a calibration spectrum for several minutes – make sure the K and L electron lines and the γ -photon Compton edge are well-defined in the spectrum before saving it. In your notebook, record the MCA channel numbers of the K and L lines and the Compton edge (use the MCA software's cursor to determine these channel numbers).

Examine the O-scope display of the amplifier output pulses and record the pulse height (in volts) of the pulses corresponding to K line detections. Use the K line MCA channel number to estimate a rough keV/channel energy calibration. Record this estimate along with the HV bias voltage and amplifier *Fine Gain* settings.

Remove the ^{137}Cs calibration source (don't forget to properly manage the HV bias supply to the detector!) and return it to its storage lead brick. After reassembling the detector-preamp components, get several ^{133}Ba gamma rod sources (the same ones you used for Experiment 30a) and place them around the vacuum chamber near the detector. Use the tray on top of the magnet pole piece gap to support them.

Take a long (about 20 minutes or longer) ^{133}Ba calibration spectrum. Make sure that you can identify a weak full-energy peak from the 356 keV γ -photon before stopping the calibration spectrum acquisition. In your notebook, record the MCA channel numbers of prominent calibration features you see.

Pump down the vacuum chamber

The HV bias must be removed from the detector as the vacuum system is pumped down or returned to atmospheric pressure!

Applying voltage to the detector as the pressure changes can result in sparking and arcing and can cause permanent damage to the detector.

The pressure must be less than 40 microns Hg before the HV bias may be safely applied!

Make sure all screws holding the detector flange in place are snug. Disable the HV Supply bias voltage output and then disconnect the preamp from the detector. Double-check that the ^{137}Cs calibration source has been removed from the vacuum chamber. Apply power to the vacuum pump. Monitor the vacuum gauge to ensure that the pressure in the chamber is falling.

Calibrate the Hall probe by following the procedure on page 21-10. Insert the Hall probe in the access slot on top of the magnet pole pieces; you must reposition the tray used to support the ^{133}Ba gamma rod sources to access the Hall probe slot. Make sure the calibration magnet is stored far from the apparatus electromagnet.

If the pressure seems to have stopped decreasing at some value >30 microns, ask your TA and the lab administrator for assistance – the vacuum pump may need to be vented momentarily to improve its pumping efficiency.

Once the chamber pressure is definitely remaining below 30 microns, reconnect the preamp to the detector and apply the HV bias voltage.

K line magnetic field measurements

Budget your lab time wisely as you collect this set of *K* line data; make sure you will have at least 20 minutes to perform the final procedure step to collect several different β electron data points.

Use your results from Prelab Problem 4 to find the magnetic field setting which causes *K* conversion electrons to reach the detector. When you get close to the proper magnetic field setting you should see a peak build in an MCA spectrum at the same channel number which corresponded to the *K* line feature in your ^{137}Cs calibration spectrum. Determine the pulse height voltage for these *K* conversion electrons using the oscilloscope, and then set the upper and lower limit voltages on the SCA to a small range around this voltage (a few 10ths of a volt range around the pulse height voltage).

Set up and activate the Scaler to acquire counts of *K* line events for about 10 seconds. Given the total counts displayed, what should be the approximate uncertainty in this count number? Repeat the measurement using the Scaler a couple of times and compare the observed fluctuation in the count values to your uncertainty estimate.

Slightly adjust the magnetic field (only about a 1 Gauss change) and repeat the Scaler measurement. Recording the magnetic field v. Scaler count data, make further adjustments until you find the magnetic field value which approximately maximizes the Scaler count value. Take another couple of magnetic field v. count combinations so that you have enough data to fit to determine the magnetic field which would maximize the *K* line detection rate.

Acquire β electron magnetic field v. energy data

Now set various values of the magnetic field so that you acquire several MCA spectra covering the β electron energy range (those β electrons with $Q = 514 \text{ keV}$, see Figure 4). In your notebook, record the magnetic field value along with the MCA channel number of the center of the electron peak (use the MCA software's cursor to determine the channel number). Note from Figure 4 that few electrons are emitted with kinetic energies near the maximum energy Q , so acquiring good data for these electrons can take quite a long time. If you have time, also get data for the L conversion electrons.

Secure the apparatus

The HV bias must be removed from the detector before turning off the vacuum pump!

Double check that you have the data you need! Try reloading several of your saved MCA spectra to check that they were saved properly.

Disable the HV bias to the detector. Disconnect the preamp from the detector. Disconnect power from the vacuum pump (it will take many minutes for the vacuum chamber to return to near atmospheric pressure).

Reduce the electromagnet current to zero and place the Hall probe in the calibration magnet. Record the Hall probe voltage and compare it to what you had recorded during your probe calibration. What will you do if the voltage is now several percent different from what it was during the original calibration?

Check with your TA to make sure that the equipment is properly secured before leaving the lab.

PRELAB PROBLEMS

1. MCA energy spectra of ^{137}Cs and ^{133}Ba obtained using the experiment apparatus are shown in Figure 10 below. The gain settings were the same for both spectra, so a given channel number corresponds to the same energy in each (note, however, that the range of channels plotted is different for the two spectra). These spectra are similar to those you will collect in order to calibrate the system's MCA channel number v. energy. The information in this experiment's *Appendix A: Useful Numerical Data* should prove helpful as you answer the following:
 - a. Identify the features corresponding to K ($1s$) and L ($2s$) conversion electron detections in the ^{137}Cs spectrum. Approximately what channel number corresponds to the K conversion electron energy? What then is the approximate keV/channel calibration of the x-axis?
 - b. Identify the feature in the ^{137}Cs spectrum which corresponds to the 0.6616 γ -photon. Given the atomic number of silicon, do you expect to see a strong full-energy peak for this photon? Which area of the spectrum should contain the β electrons whose $Q = 0.514\text{MeV}$?

(PROBLEMS ARE CONTINUED ON THE NEXT PAGE)

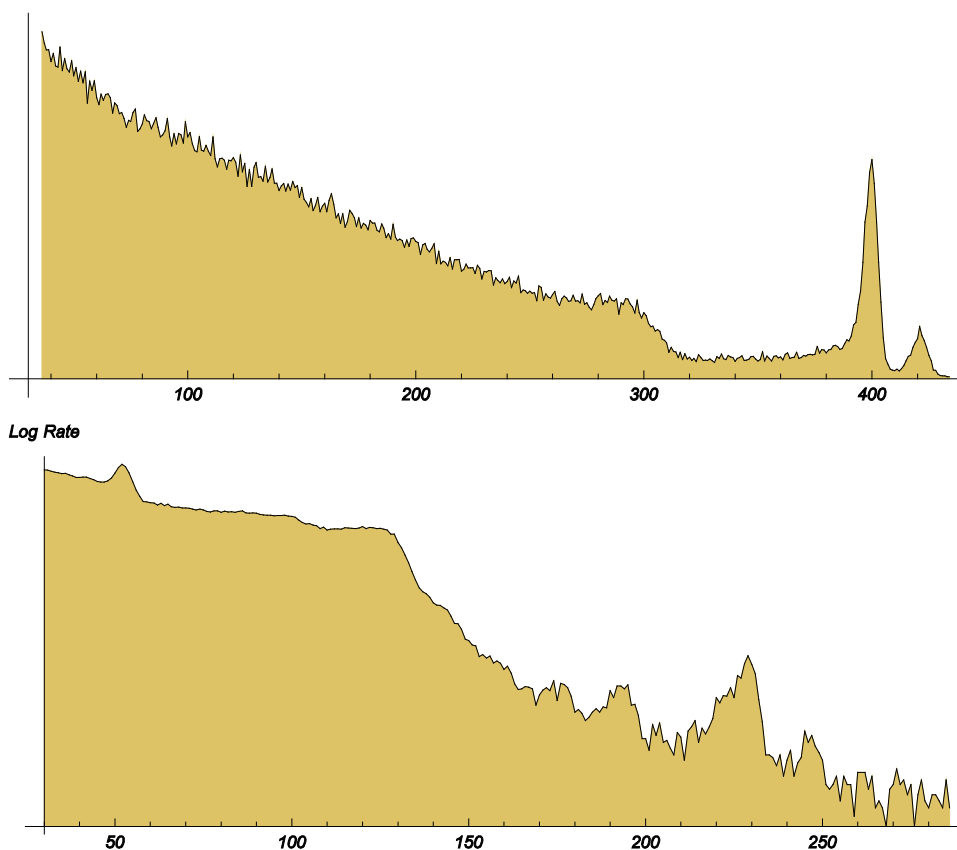


Figure 10: Counts v. energy histograms for ^{137}Cs (top) and ^{133}Ba (bottom). The cesium spectrum includes detections of electrons (β and conversion) as well as γ -photons from the source; the barium spectrum shows only γ -photons. The x-axis is MCA channel number; the vertical axis is the event count for each channel (log count for the barium spectrum).

- c. The ^{133}Ba spectrum in Figure 10 shows at least 3 γ -photon full-energy peaks, though most are quite weak. Using your rough channel energy calibration result from part (b) and the ^{133}Ba decay scheme (Fig. A-1 on page 21-A-1), identify at least 3 full-energy peaks and a Compton edge you could then use for a more accurate energy calibration (make sure you state the γ -photon energy associated with each feature you identify).
2. Derive equation (21-1) on page 1. Start with the expressions from *General Appendix A: Relativistic Kinematics* (using *energy units*, where $c \equiv 1$):

$$m^2 = E^2 - p^2 \quad \text{and} \quad T = E - m$$

Make sure to express your final result using *physical units*, with the speed of light c explicitly shown as in (21-1).

3. The relativistic momentum of a particle is given by $\vec{p} = \gamma m \vec{v}$ where $\gamma = (1 - v^2/c^2)^{-1/2}$ is the particle's *boost* (General Appendix A, equation A-6). Show that for the case of a magnetic field acting on a charged particle, the Lorentz force (21-2) will result in $dp/dt = \gamma m dv/dt$ for the time rate of change of p , even though the boost γ is a function of v . Use this result to derive expression (21-3) for the Larmor radius (also called the *cyclotron radius*).
4. Show that the functional relationship between an electron's kinetic energy T and the magnetic field strength B required to detect it using the apparatus in Figure 2 is such that B^2 can be expressed as a polynomial in the electron kinetic energy T : 1st order for Newtonian mechanics, 2nd order for relativistic mechanics.

Answer (SI units):

$$\begin{array}{l} \text{Newtonian: } B^2 = \left(\frac{2m_e}{R_{\text{eff}}^2 q_e^2} \right) T \\ \text{relativistic: } B^2 = \left(\frac{2m_e}{R_{\text{eff}}^2 q_e^2} \right) T + \left(\frac{1}{R_{\text{eff}}^2 q_e^2 c^2} \right) T^2 \end{array} \quad (21-5)$$

where q_e = the magnitude of the electron charge, m_e = electron mass, R_{eff} = effective radius of the magnetic field.

5. Assume that the magnet used for this experiment has an effective field radius of $R_{\text{eff}} = 6.9$ cm. With the electron $m_e c^2 = 0.511$ MeV, at what value for B (in Gauss = 10^{-4} Tesla) would you expect to detect the ^{137}Cs K (I_s) conversion electron: (a) using Newtonian mechanics; (b) using relativistic mechanics? See this experiment's *Appendix A: Useful Numerical Data* for the value of the K line electron kinetic energy (answers: 386G, 490G).

ANALYSIS

The purpose of your analysis is to evaluate the validity of the relativistic expression (21-1), repeated below, relating the kinetic energy T and momentum p of, in this case, the electron. In particular, you should provide a quantitative evaluation of whether the relativistic expression provides a more accurate model of the relationship between T and p than does the more familiar Newtonian model, $p^2 = 2mT$.

$$p^2 = 2mT \left(1 + \frac{T}{2mc^2} \right) \quad (21-1)$$

Your answer to Prelab problem 4, deriving equations (21-5), translates the relativistic and Newtonian expressions into your actual data: magnetic field B vs. kinetic energy T . We repeat these expressions here:

$$\begin{aligned} \text{Newtonian: } B^2 &= \left(\frac{2m_e}{R_{eff}^2 q_e^2} \right) T \\ \text{relativistic: } B^2 &= \left(\frac{2m_e}{R_{eff}^2 q_e^2} \right) T + \left(\frac{1}{R_{eff}^2 q_e^2 c^2} \right) T^2 \end{aligned} \quad (21-5)$$

These SI expressions are a little bit inconvenient to use as written, because T is better expressed in, say, MeV, and the electron mass is more conveniently thought of in terms of its rest energy $m_e c^2$, also in MeV. Your Hall probe calibration was also probably recorded in terms of Gauss, and the magnet pole piece diameter, which determines R_{eff} , is conveniently expressed in centimeters. Let's manipulate (21-5) to make use of these more convenient units.

Consider the following rearrangements of the terms in (21-5):

$$\begin{aligned} \left(\frac{2m_e}{R_{eff}^2 q_e^2} \right) T &= \frac{1}{(R_{eff} c)^2} \times \frac{2m_e c^2}{q_e} \times \frac{T}{q_e} \\ \left(\frac{1}{R_{eff}^2 q_e^2 c^2} \right) T^2 &= \frac{1}{(R_{eff} c)^2} \times \left(\frac{T}{q_e} \right)^2 \end{aligned}$$

In the final expressions, a factor of the electron charge q_e is used to divide a factor of energy (either T or $m_e c^2$). If these energies are expressed in electron volts (eV) then dividing by q_e simply changes the units from eV to V (Volts), an SI unit. Using these forms for the terms and rescaling the physical quantities in (21-5) to be more appropriate for your data (B in Gauss, T in MeV, R_{eff} in centimeters), we can rewrite (21-5) in our final form, (21-6).

Newtonian:

$$\left(\frac{B}{\text{kiloGauss}} \right)^2 = \frac{1}{\left(0.30 \frac{R_{\text{eff}}}{\text{cm}} \right)^2} \times \frac{2m_e c^2}{\text{MeV}} \times \frac{T}{\text{MeV}}$$

(21-6)

relativistic:

$$\left(\frac{B}{\text{kiloGauss}} \right)^2 = \frac{1}{\left(0.30 \frac{R_{\text{eff}}}{\text{cm}} \right)^2} \times \frac{2m_e c^2}{\text{MeV}} \times \frac{T}{\text{MeV}} + \frac{1}{\left(0.30 \frac{R_{\text{eff}}}{\text{cm}} \right)^2} \times \left(\frac{T}{\text{MeV}} \right)^2$$

The divisions by various units in these expressions mean that your data should be expressed in these units before attempting to fit B^2 v. T (i.e. energies in MeV, B in kilogauss, e.g.: $490\text{ G} = 0.49\text{ kG}$). The relativistic expression include a term quadratic in T which is not present in the Newtonian expression; it is up to you to determine which theory better represents your data. Note that if the relativistic expression is more accurate, then the ratio of the linear and quadratic coefficients of T should be consistent with twice the electron rest energy; whereas the quadratic term coefficient provides a determination of the magnet's R_{eff} .

Use your ^{137}Cs and ^{133}Ba calibration data to calibrate the MCA channel axis to energy conversion function; make sure you include Compton edges as calibration points (see equation (21-A-1) on page 21-A-1. This calibration, naturally, will introduce an element of systematic uncertainty to the energy data; similarly, uncertainty in your Hall probe calibration will systematically affect the B data. Make sure you handle these *systematic* uncertainties correctly as you perform your data analysis!

Appendix A: Useful Numerical Data

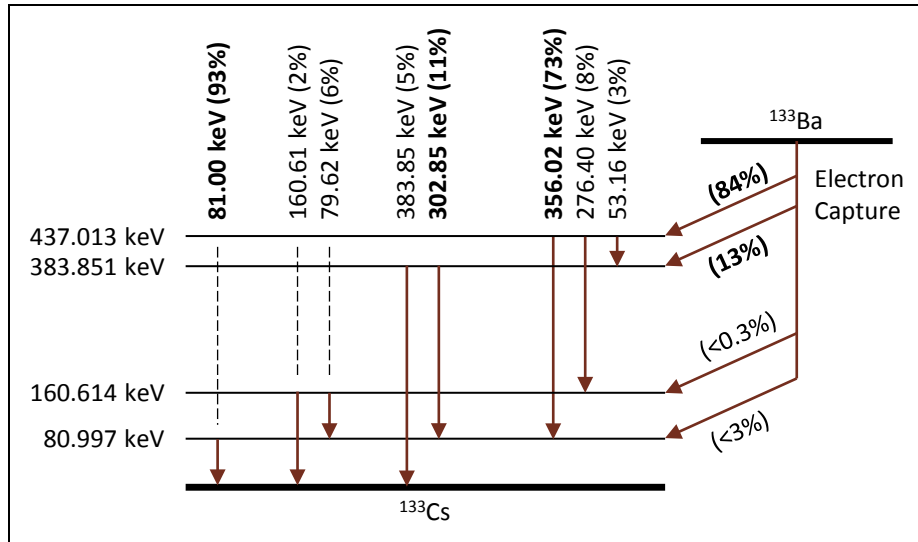
¹³³Ba calibration source

Fig. A-1: ¹³³Ba decay scheme showing γ -photon energies and emission probabilities. The β decay to ¹³³Cs is via *electron capture* (nearly always from a *1s* electron state), emitting an (undetected) electron neutrino from the proton to neutron conversion and generating an x-ray from the following *2p-1s* atomic electron transition.

¹³⁷Cs conversion electron energies

K line (1s conversion e⁻): 0.6242 MeV

L line (2s conversion e⁻): 0.6557 MeV

Compton edge energy calculation

The Compton edge energy is defined as the maximum electron kinetic energy deposited in a detector by a 180° Compton scatter of a γ -photon. This energy is given by:

$$T_{edge} = \frac{k_0}{1 + \frac{m_e c^2}{2k_0}} \quad (21-A-1)$$

where k_0 is the incoming photon energy, $m_e c^2$ is the electron rest energy (0.511 MeV), and T_{edge} is the spectrum Compton edge energy.

Silicon detector γ -photon sensitivity data

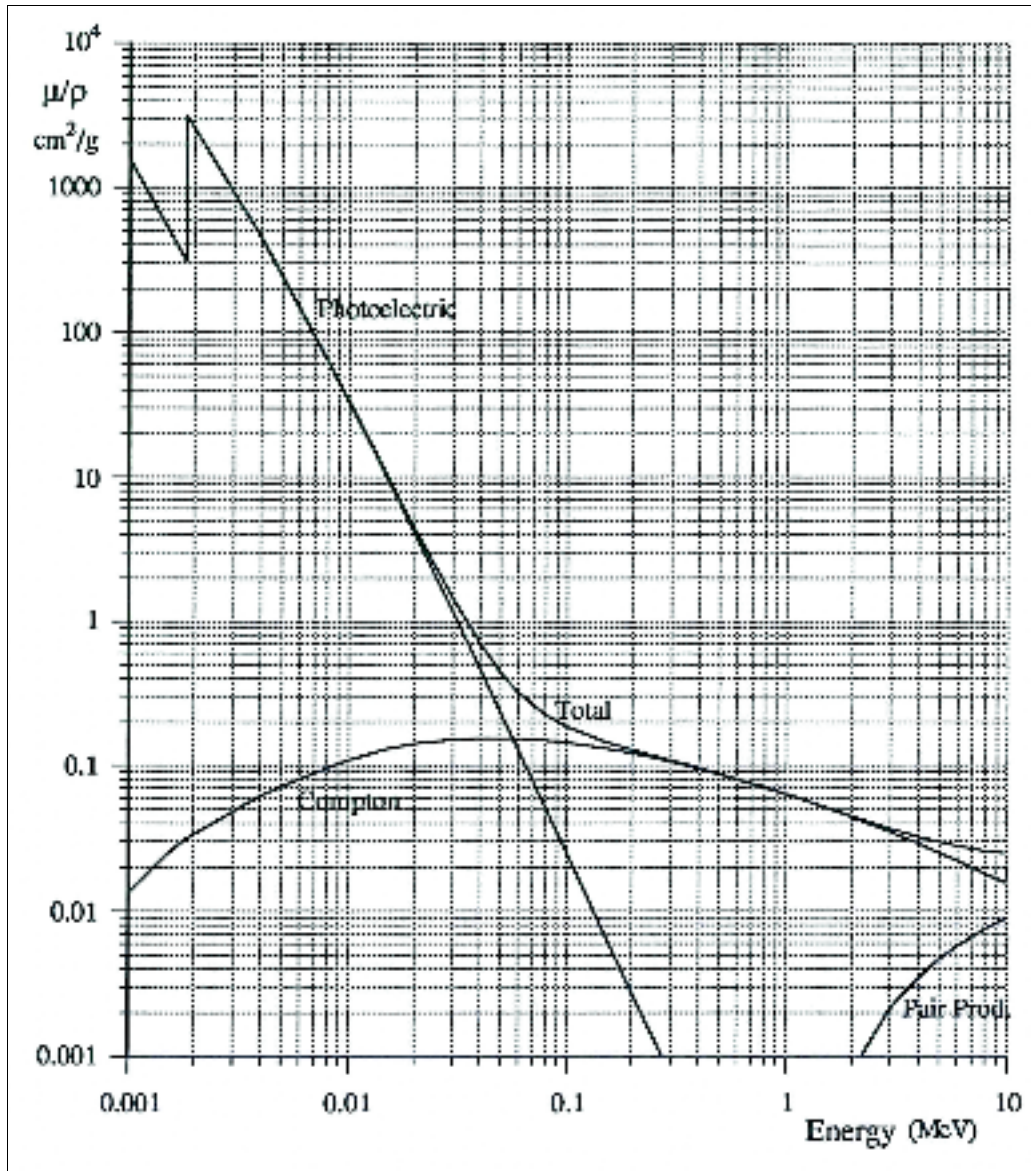


Fig. A-2: Mass attenuation coefficient data for silicon. As indicated in the plot, photoelectric absorption is unlikely for photons with energies >300 keV or so.

Silicon mass density: $2.33 \text{ gm}/\text{cm}^3$

Detector thickness: 0.3 cm